AGU PUBLICATIONS

Water Resources Research

RESEARCH ARTICLE
10.1002/2013WR014939

Key Points:
- Baseflow can be estimated continuously from surface water data
- A conceptual model was developed to accurately interpret baseflow estimates
- The approach provides a tool for assessing environmental effects on streamflow

Correspondence to:
M. P. Miller,
mamiller@usgs.gov

Citation:
Miller, M. P., D. D. Susong, C. L. Shope, V. M. Heilweil, and B. J. Stolp (2014), Continuous estimation of baseflow in snowmelt-dominated streams and rivers in the Upper Colorado River Basin: A chemical hydrograph separation approach, *Water Resour. Res.*, *50*, 6986–6999, doi:10.1002/2013WR014939.

Received 22 OCT 2013
Accepted 5 AUG 2014
Accepted article online 11 AUG 2014
Published online 26 AUG 2014

Continuous estimation of baseflow in snowmelt-dominated streams and rivers in the Upper Colorado River Basin: A chemical hydrograph separation approach

Matthew P. Miller[1], David D. Susong[1], Christopher L. Shope[1], Victor M. Heilweil[1], and Bernard J. Stolp[1]

[1]U.S. Geological Survey, Utah Water Science Center, Salt Lake City, Utah, USA

Abstract Effective science-based management of water resources in large basins requires a qualitative understanding of hydrologic conditions and quantitative measures of the various components of the water budget, including difficult to measure components such as baseflow discharge to streams. Using widely available discharge and continuously collected specific conductance (SC) data, we adapted and applied a long established chemical hydrograph separation approach to quantify daily and representative annual baseflow discharge at 14 streams and rivers at large spatial ($>$ 1000 km^2 watersheds) and temporal (up to 37 years) scales in the Upper Colorado River Basin. On average, annual baseflow was 21–58% of annual stream discharge, 13–45% of discharge during snowmelt, and 40–86% of discharge during low-flow conditions. Results suggest that reservoirs may act to store baseflow discharged to the stream during snowmelt and release that baseflow during low-flow conditions, and that irrigation return flows may contribute to increases in fall baseflow in heavily irrigated watersheds. The chemical hydrograph separation approach, and associated conceptual model defined here provide a basis for the identification of land use, management, and climate effects on baseflow.

1. Introduction

The Colorado River and its tributaries provide municipal water to approximately 40 million people in seven states and Mexico, irrigation water for over 20,000 km^2 of land, and support hydropower facilities that supply more than 4200 MW of electrical capacity [*U.S. Bureau of Reclamation*, 2012]. Additionally, the river provides recreational opportunities and critical habitat for both aquatic and terrestrial biota. To effectively manage current use and plan for future use of water, it is necessary to quantify components of the Colorado River Basin water budget. One component that is often a large fraction of total streamflow, but that is difficult to measure, is baseflow. For the purposes of this study, baseflow is defined as water that sustains flow in a river during low-flow time-periods, but is also a component of streamflow during high flow conditions, that is composed primarily of groundwater.

Quantitative estimates of baseflow in streams can be applied to address questions of baseflow response to environmental conditions. For example, daily estimates of baseflow can be used to inform scientific or management questions that require fine-scale, time-specific information, such as short-term mass balance investigations [*Burns*, 1998]. Seasonal estimates of baseflow are needed to examine questions including among-site differences in baseflow during low-flow or snowmelt conditions as a function of differences in watershed geology [*Bloomfield et al*., 2009] or hydrologic alteration due to the presence of diversions or reservoirs [*Magilligan and Nislow*, 2005]. Baseflow estimates can also be used to address questions of baseflow response to irrigation practices [*Stanton et al*., 2010] or drought [*Dahm et al*., 2003].

A common approach for quantification of different source-water components of streamflow is to use a graphical hydrograph separation approach, for which stream discharge data is the only requirement [*Nathan and McMahon*, 1990; *Wahl and Wahl*, 1988; *Eckhardt*, 2005]. One advantage of using graphical approaches for hydrograph separation is that stream discharge records are widely available, and therefore, the approach can be applied at a large number of sites, from small to large spatial scales, and extrapolated to ungauged sites. Indeed, baseflow estimates for the conterminous United States [*Wolock*, 2003; *Santhi et al*., 2008] and the entire globe [*Beck et al*., 2013] have been developed. Another approach for

quantification of different source-water components of streamflow, that has greater data requirements than the graphical approaches, and therefore is often limited to streams draining small to midsized watersheds, is a chemical mass balance approach that uses the unique chemical signatures of the source waters to separate the hydrograph. While wide application of chemical mass balance approaches is often limited by data availability, they incorporate watershed-specific geochemical information to a greater extent than approaches that rely on stream discharge data alone. Therefore, chemical mass balance estimates of baseflow are often considered to be more reliable than those from graphical hydrograph separation estimates [*Stewart et al*., 2007].

Beginning in the late 1960s, stable isotope tracers such as deuterium (δD) and oxygen-18 (δ^{18}O), and major ions such as calcium (Ca), silica (Si), sodium (Na), and specific conductance (SC), have been used to quantify surface runoff and groundwater discharge to streamflow [*Pinder and Jones*, 1969; *Dinçer, et al*., 1970]. Stable isotopes are generally considered to be the most accurate chemical tracers for hydrograph separation [*Kendall and Caldwell*, 1998]. However, the analytical costs associated with these constituents often limit their use in large studies. In a comparison of hydrograph separations conducted using geochemical tracers; *Cassie et al*. [1996] demonstrated that SC was the most effective single parameter for quantifying the runoff and groundwater components of total streamflow.

Of the chemical constituents commonly used to separate hydrographs, SC is unique in that it can be measured in situ continuously, thereby providing an opportunity for high-frequency hydrograph separation at a low cost. Continuous SC data have been used to successfully quantify two source-water end-members in a variety of stream ecosystems including snowmelt-dominated watersheds [*Covino and McGlynn*, 2007], urban watersheds [*Pellerin et al*., 2007], and a range of other settings [*Stewart et al*., 2007; *Sanford et al*., 2011; *Lott and Stewart*, 2012]. Most chemical hydrograph separation studies have been conducted in small watersheds and for short durations (e.g., storm events), although some continuous chemical hydrograph separations have been conducted for periods of 1–4 years [*Stewart et al*., 2007; *Sanford et al*., 2011]. Numerous studies have quantified two or more source-water end-members in snowmelt-dominated streams [*Caine*, 1989; *Sueker et al*., 2000; *Liu et al*., 2004; *Covino and McGlynn*, 2007]. However, to our knowledge, the use of chemical hydrograph separation to continuously estimate the runoff and baseflow components of total streamflow in snowmelt-dominated streams in large watersheds and for a long duration (2+ years) has not been reported.

The purpose of this study is to present an approach that estimates baseflow discharge to streams draining large snowmelt-dominated watersheds that range in size from 1000 to >60,000 km^2 using a well-established two component chemical hydrograph separation approach applied to long-term discharge and SC records. A conceptual model of source-water components of snowmelt-dominated streams and rivers in the Upper Colorado River Basin (UCRB) was developed to provide a framework from which the patterns in baseflow estimates can be interpreted at large temporal and spatial scales. Source waters were lumped into two end-member components: runoff and baseflow (defined in the following sections), and stream hydrographs were separated into runoff and baseflow components at a daily time step for the period of record (up to 37 years). Annual and seasonal (snowmelt and low-flow time-periods) baseflow volumes were calculated from mean daily baseflow hydrographs. Examples of how the annual and seasonal baseflow volume estimates could be used to investigate the relationships between baseflow and land use or management activities at the large watershed scale are discussed.

2. Conceptual Model

Understanding the physical processes that control how water that enters the watershed as precipitation ultimately discharges to the stream is a topic that has been studied by hydrologists for decades. The level of detail with which runoff processes and sources are identified and quantified, and in turn, the number of end-members examined, varies depending on the spatial and temporal scale of interest in a particular study. For example, *Inamdar et al*. [2013] used end-member mixing analysis (EMMA) to identify temporal variation in eleven distinct streamflow end-members in a small forested watershed in the mid-Atlantic US. Quantification of end-members at this level of detail provides much needed insight into hydrologic partitioning, processes, and streamflow response to variable watershed conditions. However, as the temporal and spatial extents of studies increase, so does the level of difficulty associated with identifying greater

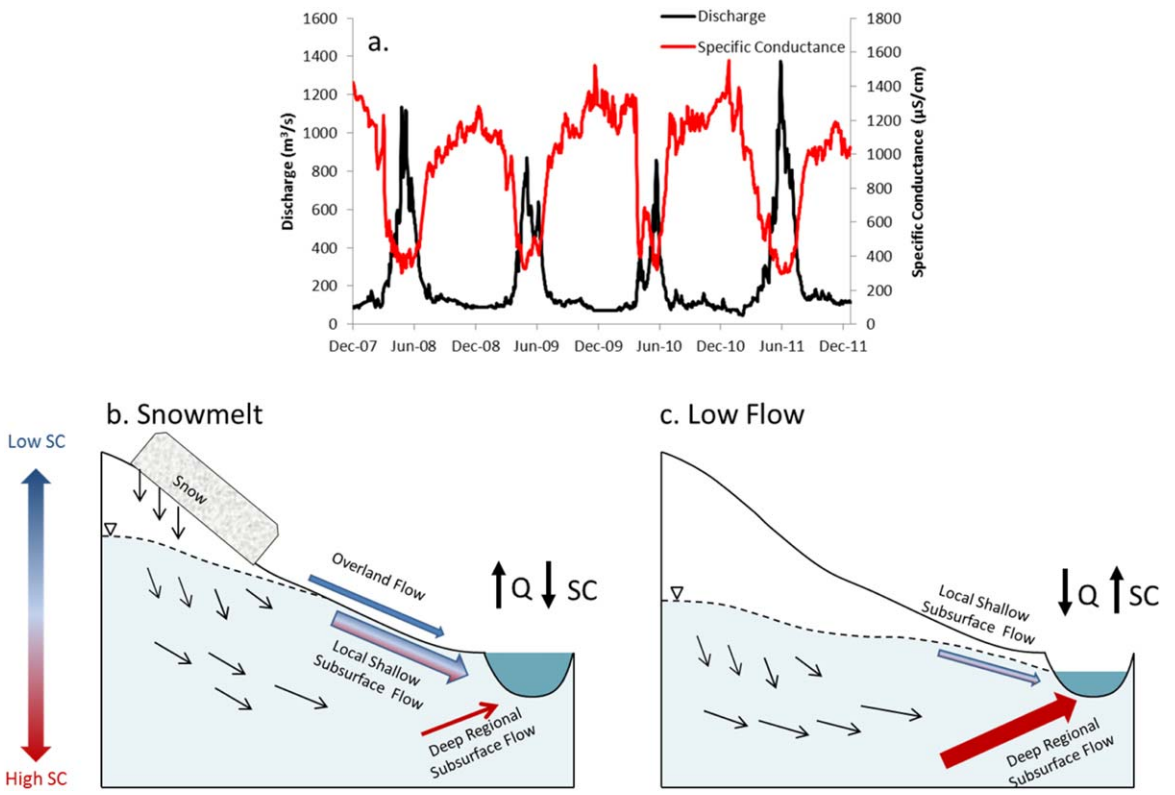

Figure 1. Conceptual model of source waters contributing to snowmelt-dominated streams. (a) Example data from CO1—there is a yearly pattern in in-stream discharge (Q) and specific conductance (SC), with (b) peak Q and minimum SC being observed during snowmelt conditions (late spring through early summer) and (c) minimum Q and peak SC being observed during low-flow conditions (late summer through early spring). Low SC overland flow and local shallow subsurface flow are the dominant flow paths contributing to the stream during snowmelt in Figure 1b. There is year-round high SC deep regional subsurface discharge to the stream, with the greatest relative contribution occurring during low-flow conditions in Figure 1c.

numbers of end-members. When quantifying source waters at broad spatial scales (e.g., multiple watersheds within the UCRB), separation of the hydrograph into many end-members is not practical, and a coarse-scale separation using two end-members is warranted. Previous studies have suggested that separation of the hydrograph into two end-members is more appropriate for large watersheds, as compared to smaller watersheds, where greater than two end-members should be considered [*Uhlenbrook et al.*, 2002].

A conceptual understanding of the multiple flow paths that contribute to stream discharge and water quality is useful for interpreting the results of hydrograph separation. These flow paths include, but are not limited to, direct precipitation, overland flow (infiltration excess or saturation overland flow), and subsurface flow. Subsurface flow paths vary in scale from local shallow-flow paths to long regional deep flow paths. Compared with shallow-flow paths, the deeper regional flow paths respond more slowly to climate and anthropogenic activities, and often have greater concentrations of dissolved constituents due to longer contact times with subsurface materials [*Winter et al.*, 1998]. In general, direct precipitation and overland flow are the temporally quickest flow paths, followed by shallow subsurface flow, and slower moving intermediate to deep regional flow. Given the small surface area of streams as compared to the surrounding watershed, the contribution of direct precipitation to streams is generally small, and therefore is ignored in our conceptual model.

Discharge peaks and SC reaches a minimum value in the late spring or early summer in snowmelt-dominated watersheds (Figure 1a). At this time, the stream water has a greater contribution from low SC source waters relative to deeper groundwater sources (Figure 1b). During times of low-flow and high in-stream SC, from late summer through early spring, groundwater flow is expected to be the dominant source-water component contributing to streamflow, with lesser contributions from shallow subsurface

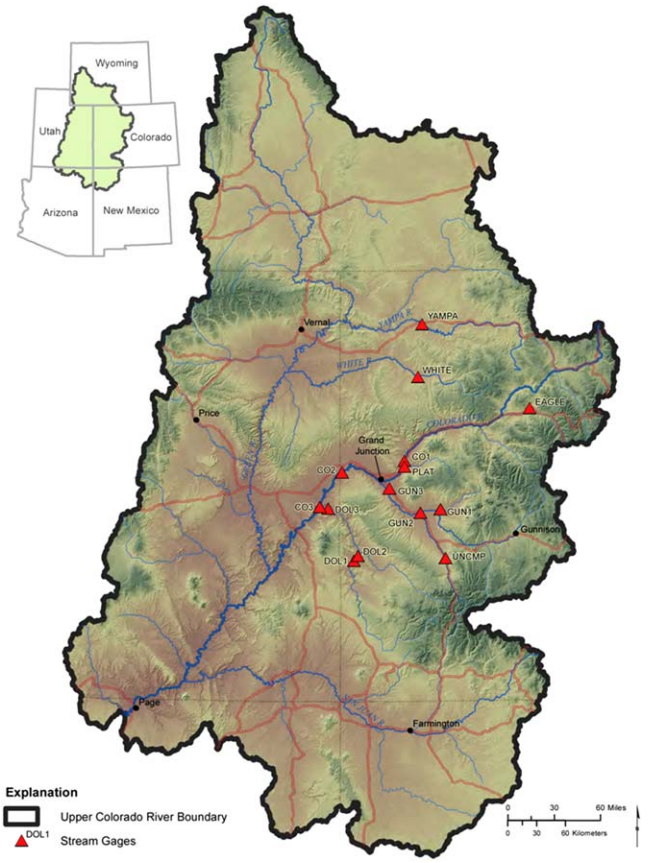

Figure 2. Map showing the Upper Colorado River Basin (UCRB) and the sampling locations for the 14 stream sites included in the study. The inset shows the location of the UCRB in the western United States.

flow (Figure 1c). This conceptual understanding provides a framework from which the runoff and baseflow end-members can be defined. The runoff end-member is low SC water that is delivered to the system during the snowmelt time period, and includes melted snow that picks up solutes on its way to the stream. Therefore, the runoff end-member is expected to be more geochemically evolved than freshly melted snow, and will have a SC concentration that is greater than that of snow ($<$10 μS/cm) [*Williams and Melack*, 1991], but less than that of the water in the stream during snowmelt; which includes inputs from high SC deep regional flow. The baseflow end-member represents the integrated SC signal from all subsurface water entering the stream and is high SC groundwater (Figures 1c). Irrigation return flow, which is irrigation water that is not used by plants and later returned to the stream, may also contribute substantial flow and SC to the stream during low-flow conditions in heavily irrigated watersheds, and is therefore included in the baseflow end member estimates.

3. Methods

3.1. Data Sources and Site Description

The UCRB is located on the western side of the continental divide, encompasses parts of five states, and drains an area of 294,000 km^2 (Figure 2). Fourteen sites draining snowmelt-dominated watersheds $>$ 1000 km^2 within the UCRB that have nearly complete (i.e., short data gaps generally $<$1 month) yearly records of continuous discharge and SC data are included in this study (Figure 2 and Table 1). Snowmelt-dominated watersheds are defined as sites where there is a peak in discharge during snowmelt in late spring or early summer that is approximately an order of magnitude greater than low-flow conditions, which persist from late summer until late spring. There is an inverse relationship between SC and stream discharge described by a power function at these sites (Figure 3a). An additional six sites draining watersheds $>$ 1000 km^2 and with nearly complete records of continuous discharge and SC are located within the UCRB, but are not included in the study. These six sites are either heavily influenced by anthropogenic activities, such as being located directly downstream of large reservoirs or diversions, for example, or have discharge patterns that are not consistent with snowmelt-dominated systems (e.g., monsoonal-dominated hydrology). Direct impacts from anthropogenic activities can alter the natural hydrologic processes such that there is not a consistent inverse relationship between discharge and SC. Accordingly, SC-based hydrograph separation approaches are often not appropriate for these systems. Figure 3b shows the SC and discharge relationship at a representative site that does not have an inverse relationship between

Table 1. Descriptive Information for UCRB Sampling Locations

Site ID	Site Name	Period of Record	Drainage Area (km^2)	Mean Discharge (m^3/s)	Mean Specific Conductance (μS/cm)	Irrigated Area[a] (km^2)	Reservoir Storage[b] (x10^7 m^3)
UNCMP	Uncompahgre River at Colona, CO	2010–2012	1,160	6.63	529	39 (3.4%)	10 (4)
PLAT	Plateau Creek Near Cameo, CO	1996–2012	1,533	5.35	585	52 (3.4%)	7.4 (54)
EAGLE	Eagle River Below Milk Creek Near Wolcott, CO	2007–2012	1,554	15.0	740	1.6 (0.1%)	6.2 (13)
GUN1	North FK Gunnison River Above Mouth NR Lazear, CO	2010–2012	2,510	14.0	930	90 (3.6%)	4.1 (40)
WHITE	White River Below Meeker, CO	1978–1983	2,652	20.4	543	67 (2.5%)	1.1 (12)
DOL1	Dolores River at Bedrock, CO	1980–2012	5,245	8.27	857	8.0 (0.2%)	51 (14)
DOL2	Dolores River Near Bedrock, CO	1980–2012	5,561	8.72	3,397	17 (0.3%)	51 (15)
YAMPA	Yampa River Near Maybell, CO	1993–2012	8,762	43.0	475	178 (2.0%)	17 (70)
DOL3	Dolores River Near Cisco, UT	2007–2012	11,862	12.6	1,190	99 (0.8%)	55 (37)
GUN2	Gunnison River at Delta, CO	2010–2012	14,597	41.7	603	407 (2.8%)	140 (147)
GUN3	Gunnison River Near Grand Junction, CO	1976–2012	20,520	68.6	847	721 (3.5%)	150 (205)
CO1	Colorado River Near Cameo, CO	1983–2012	20,684	115	882	318 (1.5%)	450 (158)
CO2	Colorado River Near Colorado-Utah State Line	1980–2012	46,229	188	961	1,247 (2.7%)	600 (437)
CO3	Colorado River Near Cisco, UT	2007–2012	62,419	187	983	1,350 (2.2%)	660 (480)

[a]The percent of total watershed area that is irrigated is shown in parentheses.
[b]The number of reservoirs in the watershed is shown in parentheses.

discharge and SC—The Green River near Greendale UT, which is located 0.8 km downstream from the Flaming Gorge Dam (capacity of 4.7 $\times$ 10^9 m^3; http://www.usbr.gov/).

Daily mean stream discharge and SC data were obtained from the U.S. Geological Survey (USGS) National Water Information System (NWIS) database. Drainage areas at the study sites range from 1160 km^2 at UNCMP to 62,419 km^2 at CO3, periods of record range from 3 years (multiple sites) to 37 years at GUN3, and mean discharge and SC for the periods of record range from 5.4 m^3/s at PLAT to 188 m^3/s at CO2 and 475 μS/cm at YAMPA to 3397 μS/cm at DOL2, respectively (Table 1).

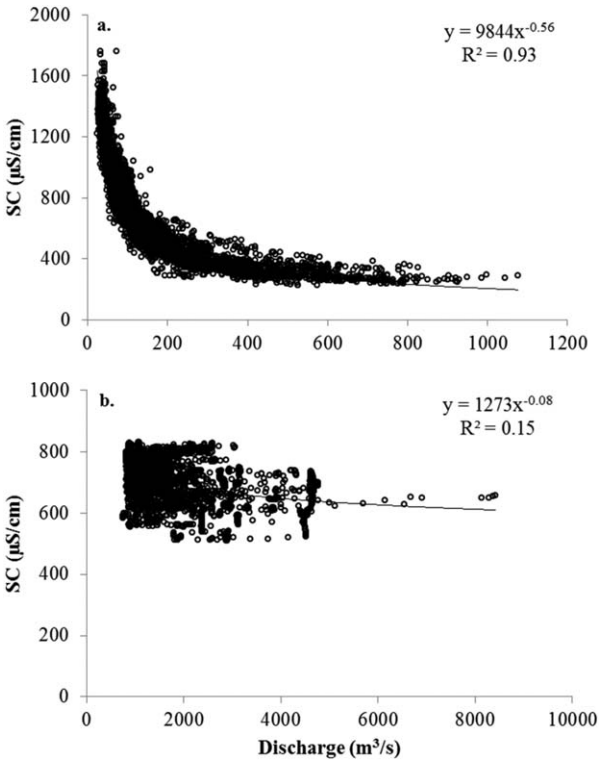

Figure 3. Examples of (a) a site (CO1) that has an inverse relationship between discharge and SC described by a power function, and (b) a site (Green River ~0.8 km downstream of the Flaming Gorge Dam) that does not have an inverse relationship between discharge and SC described by a power function.

Streams and rivers in the UCRB are heavily regulated and their watersheds have a range of land-use activities. The number of reservoirs in watersheds examined in this study range from 4 (UNCMP) to 480 (CO3) and store from 1.1 $\times$ 10^7 m^3 (WHITE) to 6.6 $\times$ 10^9 m^3 (CO3) of water (Table 1). Irrigated agriculture is common in the UCRB and has the potential to influence both the quantity and chemical quality of stream water. The area of irrigated agricultural land is less than 4% of the total watershed area in all watersheds, and ranges

Table 2. Frequently Used Variables and Corresponding Abbreviations

Variable	Abbreviation
Stream discharge	Q
Baseflow discharge	Q_{BF}
Specific conductance of the stream	SC
Specific conductance of the baseflow end-member	SC_{BF}
Specific conductance of the runoff end-member	SC_{RO}
Specific conductance of the runoff end-member representing direct routing of freshly melted snow to the stream	$SC_{RO\text{-}10}$
Uncertainty in baseflow discharge	W_{BF}

from 1.6 km^2 at EAGLE to 1350 km^2 at CO3 (Table 1). In the Paradox Valley, located between DOL1 and DOL2, there is a collapsed salt anticline that provides a natural source of high conductivity water to the Dolores River. Beginning in 1996, the Bureau of Reclamation (BOR) began continuously intercepting and removing much of the high conductivity groundwater before it discharges to the river [*Chafin*, 2003]. It has been demonstrated that, at GUN3, one of the more heavily irrigated watersheds (Table 1), flow-normalized salinity concentrations and loads decreased from 1989 to the late 1990s, but then leveled out until 2007 [*Schaffrath*, 2012].

3.2. Hydrograph Separation

The baseflow component of the hydrograph was estimated at a daily time step for the period of record at each site. Daily baseflow (Q_{BF}; m^3/s; Table 2) was calculated using a mass balance approach [*Pinder and Jones*, 1969]:

$$Q_{BF} = Q\left[\frac{SC - SC_{RO}}{SC_{BF} - SC_{RO}}\right] \quad (1)$$

where Q is the daily mean discharge (m^3/s), SC is the measured in-stream daily mean specific conductance (μS/cm), SC_{RO} is the specific conductance of the runoff end-member, and SC_{BF} is the specific conductance of the baseflow end-member. Q and SC are both measured values; whereas SC_{RO} and SC_{BF} are estimated.

SC_{RO} represents snowmelt-derived runoff discharging to the stream, composed of low SC source waters. To quantitatively represent this end-member, in-stream discrete SC data were obtained from two high elevation sites draining small watersheds in the headwaters of the UCRB. These sites are Cabin Creek Near Fraser, CO (elevation 9560 ft. above sea level, drainage area 12.6 km^2) and Elk Creek at Upper Station, Near Fraser, CO (elevation 9400 ft. above sea level, drainage area 4.3 km^2). SC_{RO} for all sites and at all times was defined as the average of the in-stream SC at these two sites combined during snowmelt (May and June; n = 55; SC_{RO} = 33 μS/cm). The rationale behind this approach is that the high SC groundwater contribution to high elevation streams draining small watersheds during snowmelt is minimal compared to the potentially large high SC groundwater contributions to streams in the study watersheds, which drain much larger areas (1000 to 60,000+ km^2).

There are multiple subsurface flow paths contributing to the stream at any point in time, each of which has a unique SC value. This is especially true in large watersheds, such as those included in this study. The SC measured in the stream during low-flow, high conductivity periods, when there is minimal contribution from snowmelt, can serve as a baseflow end-member. SC_{BF} represents this integrated baseflow conductivity discharging to the stream upstream of the measurement point. It is possible that anthropogenic activities over long periods of time, or year to year changes in the elevation of the water table, have resulted in temporal change in the SC of the baseflow end-member. To account for this possibility, temporally variable SC_{BF} values were calculated at each site. Specifically, to represent temporal variability in the integrated subsurface SC during low-flow and high conductivity conditions, a SC_{BF} value was calculated for each year during the period of record at each of the 14 study streams as the SC of the 99th percentile of the daily SC values for the year in question. Following the approach applied by *Sanford et al.* [2011], daily values of SC_{BF} were estimated by interpolating between the yearly SC_{BF} values. The 99th percentile approach was adopted to avoid the potential for outlier SC concentrations to be assigned as SC_{BF} concentrations, which could occur by defining the SC_{BF} end-member as the maximum SC concentrations measured each year. For example, for a four day period of near-zero flow conditions in August of 1981, measured SC at DOL2 was three times greater than SC_{BF} derived using the 99th percentile approach, and twice that of SC measured during any other portion of the 33 year period of record. Under these end-member definitions, a small percentage

(< 1%) of the days were predicted to have Q_{BF} greater than 100% of measured Q. Q_{BF} values for these days were set at 100% of total streamflow.

Application of the chemical hydrograph separation method requires that the following assumptions are made: (1) contributions from other end-members are negligible, (2) SC_{RO} and SC_{BF} are constant over the period of record, and (3) SC_{RO} and SC_{BF} are significantly different from one another [*Sklash and Farvolden*, 1979]. The assumption that contributions from other end-members are negligible is accounted for by the lumping of multiple source waters into two broadly defined end-members (see Conceptual Model section above). While there may be slight temporal variation in the SC of the runoff end-member, it is expected to be small relative to the measured in-stream SC concentrations at the 14 study sites. For example, the standard deviation associated with SC_{RO} is 10 μS/cm and the average SC of the 14 study streams is 1179 μS/cm. Therefore, using a constant value of SC_{RO} will not have a large impact on chemical hydrograph separation. As stated earlier, SC_{BF} is time variable in our models. The assumption that SC_{RO} and SC_{BF} are significantly different from one another is supported by large differences between the SC of the end-members (reported below).

To provide a quantitative estimate of the uncertainty in baseflow, 95% confidence levels were applied to the continuous SC hydrograph separations following the methods of *Genereux* [1998]:

$$W_{BF}\left[\left(\frac{f_{BF}}{SC_{RO}-SC_{BF}}W_{SC_{BF}}\right)^2+\left(\frac{f_{RO}}{SC_{RO}-SC_{BF}}W_{SC_{RO}}\right)^2+\left(\frac{-1}{SC_{RO}-SC_{BF}}W_{SC_S}\right)\right]^{1/2} \quad (2)$$

where W_{BF} is the uncertainty in Q_{BF} at the 95% confidence interval, f_{BF} is the fraction of the total flow that is baseflow, f_{RO} is the fraction of the total flow that is runoff (i.e., $1 - f_{BF}$), W_{SCBF} is the standard deviation of the highest 1% of measured SC concentrations multiplied by the t-value ($\alpha = 0.05$; two-tail) from the Student's t distribution, W_{SCRO} is the standard deviation associated with SC_{RO} (10 µS/cm) multiplied by the t-value ($\alpha = 0.05$; two-tail), and W_{SCS} is the analytical error in the SC measurement multiplied by the t-value ($\alpha = 0.05$; two-tail). The uncertainty of the instruments is <5% for SC concentrations less than 100 μS/cm and <3% for SC concentrations greater than 100 μS/cm [*Wagner* et al., 2006]. Analytical error was set at a constant value of 5% of measured SC when SC was < 100 μS/cm and 3% of measured SC when SC was > 100 μS/cm.

3.3. Temporal Resolution of Baseflow Separation

3.3.1. Daily Period of Record Baseflow Estimates

Estimates of Q_{BF} were calculated at a range of temporal resolutions as examples of how the separation results can be presented. At the finest level of detail, daily estimates of $Q_{BF,}$ and the associated daily uncertainty in Q_{BF}, at each site were calculated for the period of record by applying the daily discharge and SC records and the SC_{RO} and SC_{BF} concentrations to equations (1) and (2). Daily estimates of Q_{BF} and W_{BF} were used to calculate mean Q_{BF} and W_{BF} values for the period of record at each site. Mean baseflow estimates for the period of record derived using a runoff end-member defined using stream data from the two high elevation streams draining small watersheds (as described above) were compared to estimates derived using a runoff end-member representative of direct routing of freshly melted snow to the stream [$SC_{RO\text{-}10} = 10$ µS/cm; *Williams and Melack*, 1991].

3.3.2. Mean Daily Baseflow Estimates for 2007–2012

Mean daily baseflow hydrographs were generated by calculating mean daily Q_{BF} values over a 6 year period of record (2007–2012) for each day of the year (i.e., mean Q_{BF} for all 6 daily Q_{BF} values estimated on 1 January, mean Q_{BF} for all six daily Q_{BF} values estimated on 2 January, etc.). Similarly, mean daily streamflow hydrographs were generated by calculating mean daily discharge for the same 2007–2012 period of record. For the purpose of generating mean daily baseflow hydrographs, SC_{RO} was held constant at 33 µS/cm, and SC_{BF} was calculated as described above, but using only data from the 2007–2012 period of record. The restricted date range (2007–2012) was adopted to provide an example of how among-site comparisons in baseflow discharge could be facilitated. A consistent date range is required for among-site comparisons because among-site differences in baseflow estimates generated from sites with different periods of record may be due to physical differences between the sites, but may also be due to temporally variable differences in baseflow. The choice of the 2007–2012 period reflects a balance between having a relatively long

Table 3. Baseflow End-Member Concentrations (SC_{BF}) and Baseflow Estimates (Q_{BF}) ± Uncertainty (W_{BF}) Derived Using Two Different Runoff End-Member Concentrations (SC_{RO}) for the Entire Period of Record at Each Site[a]

		Runoff End-Member Representative of Snowmelt Runoff (SC_{RO} = 33 μS/cm)	Runoff End-Member Representative of Direct Routing of Snowmelt to the Stream (SC_{RO-10} = 10 μS/cm)
Site ID	Mean SC_{BF} (μS/cm)	Mean Q_{BF} ± Mean W_{BF} [b] (m^3/s)	Mean Q_{BF} [b] (m^3/s)
UNCMP	625 ± 11	5.0 ± 0.3 (75%)	5.1 (76%)
PLAT	745 ± 49	3.0 ± 0.4 (56%)	3.1 (58%)
EAGLE	1,289 ± 77	3.7 ± 0.4 (25%)	3.9 (26%)
GUN1	1,445 ± 55	4.5 ± 0.2 (32%)	4.7 (33%)
WHITE	732 ± 74	11.9 ± 0.8 (59%)	12.1 (60%)
DOL1	1,792 ± 340	2.1 ± 0.2 (25%)	2.2 (26%)
DOL2	10,656 ± 8,100	1.0 ± 1.2 (11%)	1.0 (11%)
YAMPA	843 ± 145	13.4 ± 2.3 (30%)	14.3 (33%)
DOL3	2,191 ± 178	3.9 ± 0.3 (31%)	4.0 (32%)
GUN2	918 ± 43	21.6 ± 1.9 (53%)	22.1 (53%)
GUN3	1,222 ± 224	39.4 ± 5.0 (57%)	40.1 (58%)
CO1	1,335±121	54.4 ± 4.5 (47%)	55.5 (48%)
CO2	1,336 ± 165	103 ± 9.6 (55%)	104 (56%)
CO3	1,429 ± 34	93.1 ± 6.0 (50%)	94.7 (51%)

[a]Sites are listed in order of increasing drainage area.
[b]Ratio of mean baseflow to mean total streamflow during the period of record, expressed as a percentage, at each site is shown in parentheses.

record (6 years) and retaining a majority (10) of the original 14 sites. Annual, snowmelt time-period, and low-flow time-period baseflow volumes were calculated as the sum of mean daily baseflow during the entire year, the snowmelt time-period, and the low-flow time-period, respectively. The snowmelt time-period was defined by visual inspection of the mean daily streamflow hydrographs (i.e., beginning of rising limb to end of falling limb of snowmelt peak), and the low-flow period was the remainder of the year.

4. Results

4.1. Daily Period of Record Baseflow Estimates

SC_{RO}, defined as the average in-stream SC at the two high elevation sites during snowmelt, was 33±10 μS/cm. Mean SC_{BF} concentrations for the period of record ranged from 625±11 μS/cm at UNCMP to 10,656±8100 μS/cm at DOL2, where there is a collapsed salt anticline providing a naturally high source of conductivity (Table 3). For reference, the next highest SC_{BF} concentration was at DOL3 (2191±178 μS/cm). End-member concentrations were significantly different between sites with differences in mean SC_{BF} being greater than SC_{RO} by a factor of 20 at UNCMP to 320 at DOL2. Mean Q_{BF} for the period of record (using a runoff end-member of 33 μS/cm) ranged from 1.0±1.2 m^3/s at DOL2 to 103±9.6 m^3/s at CO2 (Table 3—column 3).

Daily SC and discharge for the entire period of record at CO1 are shown as an example of long-term patterns in SC and discharge at UCRB stream sites (Figure 4a). Similar to all 14 sites, discharge and SC were inversely related to one another at CO1 over the 30 year period of record (Figure 3a). Maximum and minimum SC concentrations tended to be lower during high flow years (e.g., 1983, 1997, 2011) than low-flow years (e.g., 1989, 2002, 2012). Daily baseflow estimates and associated uncertainties derived from the SC and discharge data at CO1 are shown for the period of record in Figure 4b. Q_{BF} was variable over time, with a mean Q_{BF} for the period of record of 54 ± 4.5 m^3/s (Table 3). Temporally, Q_{BF} was higher during high flow years and lower during low-flow years. Daily baseflow estimates and uncertainties for water year 2001 are shown as examples of finer temporal-scale-resolution patterns in baseflow in Figure 4c. Baseflow was relatively invariant during low-flow conditions, but increased during snowmelt. In general, uncertainty was greater during low-flow conditions as compared to during snowmelt.

When the runoff end-member was defined as that of direct routing of freshly melted snow to the stream (SC_{RO-10}=10 μS/cm), the mean baseflow for the period of record increased at all sites relative to the baseflow estimates derived using a runoff end-member defined using stream data from the two high elevation streams draining small watersheds (SC_{RO}=33 μS/cm; Table 3). However, the increase in estimated baseflow

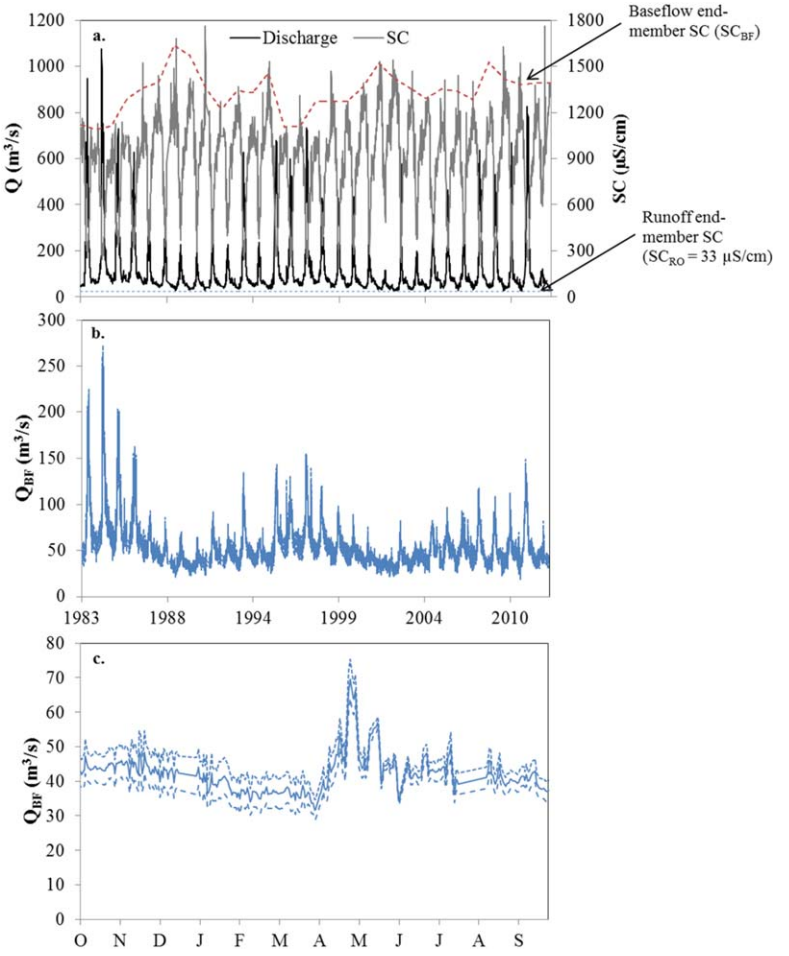

Figure 4. (a) Stream discharge (Q, black solid line) and specific conductance (SC, gray solid line) for the period of record at CO1. Upper and lower dashed lines in (a) represent the baseflow (SC_{BF}; red dashed line) and runoff (SC_{RO}; blue dashed line) end-member SC concentrations, respectively. Daily baseflow (Q_{BF}; solid line) and upper and lower daily uncertainties at the 95% confidence interval ($Q_{BF} \pm W_{BF}$; dashed lines) for (b) the period of record and (c) for a single year (water year 2001). Note that in Figure 2b, the uncertainty is small compared to the magnitude of baseflow, and therefore the uncertainty lines cannot be easily distinguished from the baseflow line.

was small and within the range of uncertainty at the 95% confidence interval calculated using the runoff end-member of 33 µS/cm.

4.2. Mean daily Baseflow Estimates 2007–2012

Mean daily discharge and baseflow hydrographs for the 2007–2012 period of record showed similar patterns for all 10 sites (Figure 5). The mean daily discharge began rising in spring (March–May), peaked in June or July, and returned to low-flow conditions in August. Discharge was low and relatively invariant for the remainder of the year (August-March). There was a noticeable peak in baseflow discharge concomitant with the rising limb of discharge in late spring at all sites; although the increase was substantially less at DOL2, where groundwater is being pumped out of the system prior to reaching the river. Mean daily baseflow increased in the fall at GUN3, and to a lesser degree at CO2 and CO3, which are located just downstream of the confluence of the Gunnison River and the Colorado River.

The annual volume of baseflow for the 2007–2012 period of record, calculated from the mean daily baseflow hydrographs, ranged from 2.8×10^7 m^3/yr at DOL2 to 3.1×10^9 m^3/yr at CO2 (Table 4). As a percentage, baseflow ranged from 21% (DOL2) to 58% (PLAT and GUN3) of annual stream discharge. Seasonally, baseflow ranged from 1.3×10^7 m^3 (DOL2) to 1.3×10^9 m^3 (CO2) during the snowmelt time-period and from 1.5×10^7 m^3 (DOL2) to 1.8×10^9 m^3 (CO2) during the low-flow time-period. As a percentage, baseflow ranged from 13% (DOL2) to 45% (GUN3) of streamflow during the snowmelt time-period and from 40% (DOL2) to 86% (PLAT) of total discharge for the low-flow time-period.

Greater than or equal to 40% of the annual baseflow volume was discharged to the stream during the snowmelt time-period (Table 4), which comprises ~25% of the year, at all sites. Seventy-eight percent of the annual baseflow was discharged to the stream during the snowmelt time-period at YAMPA, one of the sites least impacted by reservoir storage. To investigate the potential influence of reservoir storage on the timing of baseflow discharge, the volume of water stored in reservoirs normalized to watershed drainage area was plotted against the percentage of annual baseflow discharged to the stream during the snowmelt time-period (using the 2007–2012 baseflow estimates). There was a negative logarithmic relationship

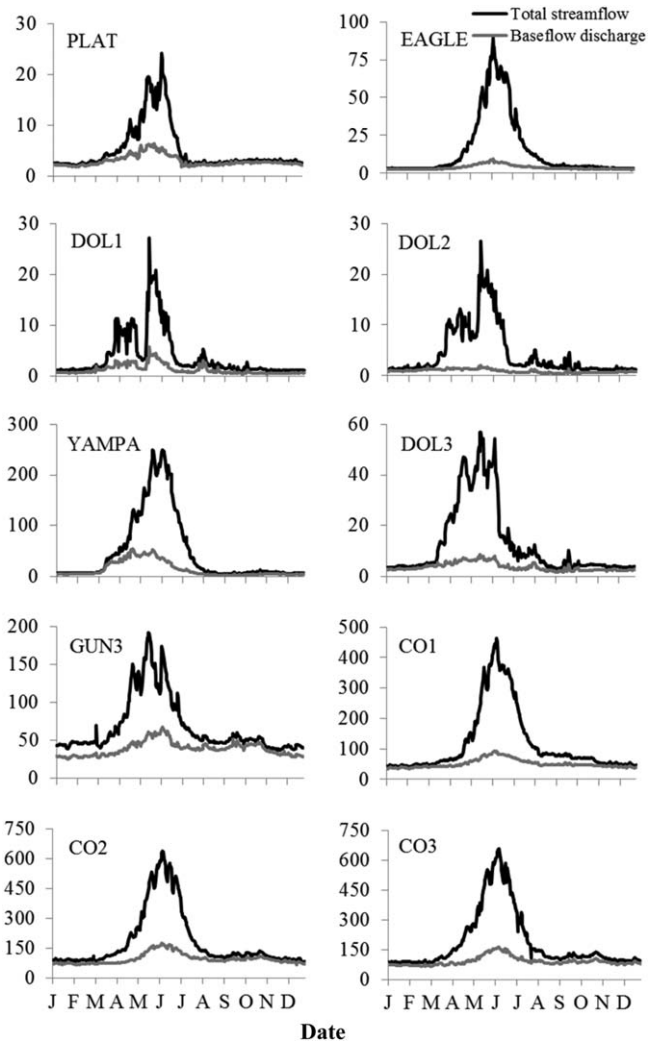

Figure 5. Mean daily hydrographs (black lines) and mean daily baseflow hydrographs (gray lines) for the 2007–2012 period of record at each site. End-member SC concentrations and the volumes of baseflow delivered to each site during snowmelt, low-flow conditions, and the entire year are shown in Table 4. Sites increase in drainage area from left to right and top to bottom.

between the volume of water stored in reservoirs normalized to watershed drainage area and the percentage of total annual baseflow discharged to the stream during the snowmelt time-period (Figure 6; $R^2 = 0.60$).

5. Discussion

The approach applied here provides quantitative estimates of daily and mean daily runoff and baseflow components of streamflow in 14 snowmelt-dominated streams and rivers at large spatial (> 1000 km^2 watersheds) and temporal (up to 37 years) scales, using widely available discharge and continuous SC data from USGS gages in the UCRB. While the two component tracer-based hydrograph separation approach used here has long been established in the literature, it has not been adapted and applied to streams draining large snowmelt-dominated watersheds for long periods of record. We utilized the unique geochemical signature of snowmelt (low SC) and groundwater (high SC) to partition channel flow into snowmelt and groundwater contributions at large temporal and spatial scales. The ability to estimate baseflow, and associated uncertainty, at a daily time step in snowmelt-dominated systems is important for a more complete understanding of the water budget in the UCRB, and provides information for addressing a variety of questions, including, climate, management, and land use impacts on the baseflow component of streams.

5.1. Source-Water Contributions to End-Members

The large spatial and temporal extents of the watersheds and data records examined here make it difficult, if not impossible, to quantify the relative contribution of numerous source waters to a stream at a given point in time; as has been done in smaller watersheds and for shorter durations using EMMA [e.g., *Christopherson and Hooper*, 1992; *Burns et al*., 2001; *Inamdar, et al*., 2013]. Examination of end-member SC concentrations provides some insight into source waters contributing to the runoff and baseflow end-members. If freshly melted snow were the only source water contributing to the stream during snowmelt, then SC_{RO}, which is defined as 33 μS/cm at all sites, would be expected to be similar to that of snow [< 10 μS/cm; *Williams and Melack*, 1991]. The definition of SC_{RO} is three times that of snow to indicate that direct routing of snowmelt to the stream is not the only contributor to the runoff end-member. Rather, snow flows on and infiltrates the land surface as it melts, and picks up solutes on its way to the

Table 4. Summary Statistics for 2007–2012 Period of Record at Each Site[a]

Site ID	Annual Baseflow (m^3)	Snowmelt Period Baseflow (m^3)	Low-Flow Period Baseflow (m^3)	Percentage of Yearly Baseflow During Snowmelt
PLAT	9.4×10^7 (58%)	4.4×10^7 (43%)	4.9×10^7 (86%)	47%
EAGLE	1.2×10^8 (25%)	6.9×10^7 (17%)	4.6×10^7 (71%)	60%
DOL1	3.9×10^7 (33%)	2.3×10^7 (27%)	1.6×10^7 (47%)	59%
DOL2	2.8×10^7 (21%)	1.3×10^7 (13%)	1.5×10^7 (40%)	47%
YAMPA	4.7×10^8 (30%)	3.6×10^8 (27%)	1.0×10^8 (58%)	78%
DOL3	1.2×10^8 (30%)	6.0×10^7 (20%)	6.3×10^7 (54%)	49%
GUN3	1.2×10^9 (58%)	5.7×10^8 (45%)	6.6×10^8 (77%)	46%
CO1	1.6×10^9 (44%)	6.9×10^8 (29%)	9.1×10^8 (72%)	43%
CO2	3.1×10^9 (53%)	1.3×10^9 (36%)	1.8×10^9 (80%)	42%
CO3	2.9×10^9 (50%)	1.2×10^9 (33%)	1.7×10^9 (77%)	41%

[a]The amount of baseflow for the specified time-period is shown in columns 2–4, with the fraction of total streamflow that is baseflow during that time period in parentheses. The fraction of the total annual baseflow that enters the stream during the snowmelt time period is shown in the last column. Sites are listed in order of increasing drainage area.

stream [*Stottlemyer and Troendle*, 1999; *Stottlemyer*, 2001]. Comparison of baseflow estimates derived using SC_{RO} defined using stream data from the two high elevation streams draining small watersheds (SC_{RO}=33 μS/cm), with baseflow estimates derived using $SC_{RO\text{-}10}$, representing direct routing of snow to the stream, demonstrates that the difference between these two approaches is within the uncertainty of the baseflow estimates.

The high within- and among-site variability in SC_{BF} indicates temporal and spatial variability in source waters comprising the baseflow end-member. The fact that multiple source waters contribute to the baseflow end-member (see Figure 1c), and that there is likely temporal variability in the relative contribution of each source water to the end-member, makes it impossible to identify a single independent subsurface SC concentration (from a single groundwater well, for example) that can be used to define SC_{BF}. It is for this reason that we used the in-stream SC data during low-flow conditions, when snowmelt was not contributing to stream discharge, to characterize the baseflow end-member. In a survey of 815 samples collected from 328 groundwater wells located in a variety of geological formations and along different flow paths in the Yampa River watershed, SC ranged from 50 to 15,900 μS/cm, with a median concentration of 1170 μS/cm [*Bauch et al*., 2012]. This large range in SC concentrations serves as an example of the within-watershed variability in groundwater SC concentrations that are present in large watersheds, such as those included in this study. If a single well, or small number of wells, were sampled and used as independent measures of the baseflow end-member, it is possible that a concentration that is not representative of an integration of all subsurface source waters discharging to the stream could be chosen as the baseflow end-member (anywhere from 50 to 15,900 μS/cm in this example). The fact that the median value of 1170 μS/cm is similar to our estimated average SC_{BF} at the YAMPA site of 843±145 μS/cm provides some confidence in the assumption that SC_{BF} is representative of an integrated SC signal of all subsurface source waters discharging to the stream.

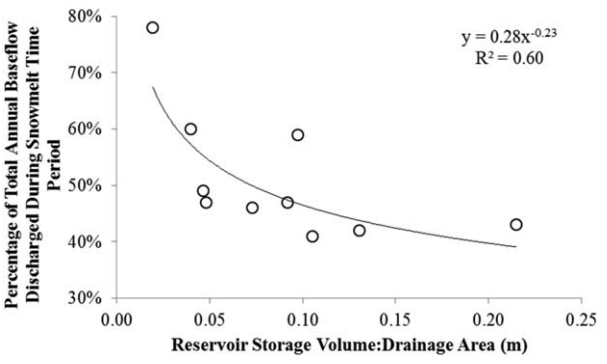

Figure 6. Percentage of total annual baseflow discharged during the snowmelt time-period (2007–2012 period of record) as a function of the volume of water stored in reservoirs normalized to watershed drainage area.

Potential drivers of among-site spatial variability in source waters include regional differences in geology, point sources, and/or land use practices that interact to influence the relative proportions of different source waters contributing to the baseflow end-member. For example, the mean SC_{BF} value of 10,656 at DOL2, which is ~5–20 times the SC_{BF} concentration at other sites, is a result of the presence of the collapsed salt anticline (a pseudo-

point source) in the Paradox Valley. This site also serves as an example of the importance of having time variable and spatially variable baseflow end-members. The pumping to intercept high SC groundwater prior to reaching the stream, which began in 1996—approximately half way through the period of record at DOL2—has resulted in a temporal change in the SC of the baseflow discharging to the stream. This variability is accounted for by having a time variable baseflow end-member, and is reflected in the high standard deviation of SC_{BF} at DOL2. Similarly, salinity control projects in other parts of the UCRB have been suggested as management actions that alter baseflow SC, and subsequently, in-stream SC concentrations. A decrease in flow-normalized salinity concentrations and loads at GUN3 from 1989 to the late 1990s was identified and attributed, at least in part, to the implementation of salinity control projects which began in the late 1980s [*Schaffrath*, 2012]. If the baseflow end-member at GUN3 was not time-variable, it would be impossible to differentiate the relative importance of temporal change in baseflow discharge to a stream from temporal change in the chemistry of the baseflow end-member (i.e., decreased contributions of highly saline irrigation return flow water to the baseflow end-member). While temporal patterns in baseflow are not investigated as part of this study, the approach of using temporally variable baseflow end-members will be useful for future studies that aim to quantify temporal changes in baseflow.

5.2. Relations Between Baseflow, Land Use, Management, and Climate

The chemical hydrograph separation approach for estimating baseflow, along with the baseflow estimates for the 14 streams in the UCRB presented here, serve as an example of how the approach could be used in future studies to address a variety of important questions regarding land use, management, and environmental controls on baseflow. The baseflow patterns at the 10 sites for which mean daily hydrographs were generated are similar to many studies that have shown temporal variability in baseflow or "old water" components of streamflow, including increases in baseflow during snowmelt or storm events [*Hooper and Shoemaker*, 1986; *Genereux and Hooper*, 1998; *McNamara et al*., 1997; *Lott and Stewart*, 2012] due to processes such as groundwater ridging [*Sklash and Farvolden*, 1979] or transmissivity feedback [*Kendall et al*., 1999], for example. Deviation from the flat line baseflow pattern during nonsnowmelt time-periods may suggest impacts from land use or management effects. For example, the increase in baseflow in the late summer and fall at GUN3, which has the largest percentage of irrigated area of the study streams, may be indicative of unused irrigation water returning to the stream at this time. This interpretation is consistent with model results showing seasonal increases in return flows to the Arkansas River during the late summer and fall months [*Gates et al*., 2012]. Moreover, this "fall bump" at GUN3 appears to be propagated downstream, as there is also a slight increase in fall baseflow at CO2, and to a lesser degree at CO3. Alternative processes that could be driving the "fall bump" in baseflow at these sites are increased groundwater discharge to streams following snowmelt recession in response to a reversal in the hydraulic gradient as stream levels drop [*Huntington and Niswonger*, 2012], and/or increases in flow as a result of decreasing evapotranspiration at this time of year [*Wigley and Jones*, 1985].

While reservoirs can also impact the SC-based separation (see Figure 3b), we propose that SC-based separations conducted at sites far enough downstream from reservoirs, such that the discharge-SC power function relationship is upheld, can be used to accurately estimate baseflow. This is because low conductivity water that is stored in reservoirs during snowmelt, and later released, would be interpreted as baseflow by a graphical approach, but the geochemical signature (i.e., the low SC) allows for the chemical hydrograph separation to identify a portion of the reservoir release during the low-flow time-period as runoff. The among-site variability in the storage of low SC runoff water in reservoirs and/or via geologic and soil conditions, and later release of this low SC water, may be contributing to the finding that baseflow ranged from as low as 40%, but up to 86%, of streamflow during low flow conditions.

Similar to the storage of low SC runoff water, reservoirs have the potential to store baseflow that is discharged to the stream during the snowmelt time period. Of the 10 sites for which mean daily hydrographs (2007–2012) were generated, the YAMPA has the smallest volume of water stored in reservoirs normalized to watershed area, and had the greatest relative contribution of baseflow during snowmelt (78% of baseflow was discharged during snowmelt; compared with 41–60% at the other nine sites). The negative relationship between the volume of water stored in reservoirs normalized to watershed drainage area and the percentage of total annual baseflow discharged during the snowmelt time-period (Figure 6) suggests that watersheds with greater amounts of reservoir storage relative to drainage area may be retaining baseflow discharged to the system during snowmelt. If reservoirs do alter baseflow in this way, that would act to

decrease the magnitude of the baseflow "bump" during snowmelt at sites with upstream reservoir storage. Other studies have found that retention of water in reservoirs in snowmelt-dominated streams results in reduced variability in flow regimes [*Poff et al*., 2007; *Arrigoni et al*., 2010].

The among-site variability in the relative fraction of total stream discharge that is baseflow discharge, either seasonally or annually, may provide some initial insight into the sensitivity of streamflow to short-term changes in climate. For example, at sites with a greater proportion of baseflow, stream discharge may receive greater relative inputs of deep regional groundwater, and therefore, may be less sensitive to short-term changes in climate, including drought or potential shifts from snow dominated to rain dominated regimes. However, determination of site-specific sensitivity to short-term changes in climate requires information on groundwater storage, transit times, and how aquifer recharge is influenced by climate variability; none of which are provided as part of this study.

5.3. Conclusions

A chemical hydrograph separation approach has been applied successfully to estimate the baseflow component of streamflow in 14 large snowmelt-dominated watersheds in the UCRB for long periods of record (up to 37 years), using only widely available in-stream SC and discharge data. On an annual basis, for a restricted period of record, the baseflow component ranged from 21% to 58% of total annual streamflow. Baseflow ranged from 13 to 45% of streamflow during snowmelt and 40–86% of total streamflow during low-flow conditions. While data from a larger number of sites are needed to reach definitive conclusions regarding environmental effects on baseflow discharge, preliminary assessment of seasonal variations in baseflow identified patterns that may be indicative of reservoir or irrigation effects. Specifically, reservoirs may retain baseflow and/or runoff discharged to streams during snowmelt and release that water during low-flow conditions, and irrigation return flows are likely contributing to increases in fall baseflow in heavily irrigated watersheds. While these preliminary baseflow-land use relationships warrant further investigation, the approach and results described here provide a valuable tool to improve our understanding of the water budget of the UCRB and other snowmelt-dominated watersheds, and further our ability to quantitatively address relationships between baseflow, climate, land use, and management activities.

Acknowledgments

The authors are grateful to the many USGS employees who collected the samples that were used in this study. We would like to thank J. Blomquist, D. Burns, P. Capel, R. Hirsch, P. Lambert, B. Pellerin, J. Raffensperger, and J. Tesoriero for helpful feedback during the development of the study. K. Jones and S. Buto generously provided reservoir storage and irrigated acreage data. D. Wolock provided helpful comments on earlier versions of this manuscript. We are also grateful to the associated editor, two anonymous reviewers, and R. Hooper for comments on an earlier version of this manuscript. This work was funded by the U.S. Geological Survey WaterSMART and National Water Quality Assessment Integrated Watershed Studies Programs.

References

Arrigoni, A. S., M. C. Greenwood, and J. N. Moore (2010), Relative impact of anthropogenic modifications versus climate change on the natural flow regimes of rivers in the Northern Rocky Mountains, United States, *Water Resour. Res.*, *65*, W12542, doi:10.1029/2010WR009162.

Bauch, N. J., J. L. Moore, K. R. Schaffrath, and J.A. Dupree (2012), Water-quality assessment and macroinvertebrate data for the Upper Yampa River watershed, Colorado, 1975 through 2009, *U.S. Geol. Surv. Sci. Invest. Rep., 2012–5214*, 129 pp.

Beck, H. E., A. I. J. M. van Dijk, D. G. Miralles, R. A. M. de Jeu, L. A. Brijnzeel, T. R. McVicar, and J. Schellekens (2013), Global patterns in base flow index and recession based streamflow observations from 3394 catchments, *Water Resour. Res.*, *49*, 7843–7863, doi:10.1002/2013WR013918.

Bloomfield, J. P., D. J. Allen, and K. J. Griffiths (2009), Examining geological controls on baseflow index (BFI) using regression analysis: An illustration from the Thames Basin, UK, *J. Hydrol.*, *373*, 164–176, doi:10.1016/j.hydrol.2009.04.025.

Burns, D. A. (1998), Retention of NO_3^- in an upland stream environment: A mass balance approach, *Biogeochemistry*, *40*, 73–96, doi:10.1023/a:1005916102026.

Burns, D. A., J. J. McDonnel, R. P. Hooper, N. E. Peters, J. E. Freer, C. Kendall, and K. Beven (2001), Quantifying contributions to storm runoff through end-member mixing analysis and hydrologic measurements at the Panola Mountain Research Watershed (Georgia, USA), *Hydrol. Processes*, *14*, 1903–1924, doi:10.1002/hyp.246.

Caine, N. (1989), Hydrograph separation in a small alpine basin based on inorganic solute concentrations, *J. Hydrol.*, *112*, 89–101.

Cassie, D., T. L. Pollock, and R. A. Cunjak (1996), Variation in stream water chemistry and hydrograph separation in a small drainage basin, *J. Hydrol.*, *178*, 137–157, doi:10.1016/0022-1694(95)02806-4.

Chafin, D. T. (2003), Effect of the Paradox Valley Unit on the dissolved-solids load of the Dolores River near Bedrock, Colorado, 1988–2001, *U.S. Geol. Surv. Water Resour. Invest. Rep., 2002–4275*, 6 pp.

Christopherson, N., and R.P. Hooper (1992), Multivariate analysis of stream water chemical data: The use of principal components analysis for the end-member mixing problem, *Water Resour. Res.*, *28*, 99–107, doi:10.1029/91WR02518.

Covino, T. P., and B. L. McGlynn (2007), Stream gains and losses across a mountain-to-valley transition: Impacts on watershed hydrology and stream water chemistry, *Water Resour. Res.*, *43*, W10431, doi:10.1029/2006WR005544.

Dahm, C. N., M. A. Baker, D. I. Moore, and J. R. Thibault (2003), Coupled biogeochemical and hydrological response of streams and rivers to drought, *Freshwater Biol.*, *48*, 1219–1231, doi:10.1046/j.1365-2427.2003.01082.x.

Dinçer, T., B. R. Payne, T. Florkowski, J. Martinec, and E. Tongiorgi (1970), Snowmelt runoff from measurements of tritium and oxygen-18, *Water. Resour. Res.*, *6*, 110–124, doi:10.1029/WR006i001p00110.

Eckhardt, K. (2005) How to construct recursive digital filters for baseflow separation, *Hydrol. Processes*, *19*, 507–515, doi:10.1002/hyp.5675.

Gates, T. K., L. A. Garcia, R. A. Hemphill, E. D. Morway, and A. Elhaddad (2012), Irrigation practices, water consumption, and return flows in Colorado's lower Arkansas River Valley, *Color. Water Inst. Tech. Comp. Rep., 221*, 115 pp.

Genereux, D. (1998), Quantifying uncertainty in tracer-based hydrograph separations, *Water Resour. Res.*, *34*, 915–919, doi:10.1029/98WR00010.

Genereux, D., and R. P. Hooper (1998), Oxygen and hydrogen isotopes in rainfall-runoff studies, in *Isotope Tracers In Catchment Hydrology*, edited by C. Kendall and J. J. McDonnell, pp. 319–346, Elsevier, Amsterdam.
Hooper, R. P., and C. A. Shoemaker (1986), A comparison of chemical and isotopic hydrograph separation, *Water Resour. Res.*, *22*, 1444–1454, doi:10.1029/WR022i010p01444.
Huntington, J. L., and R. G. Niswonger (2012), Role of surface-water and groundwater interactions on projected summertime streamflow in snow dominated regions: An integrated modeling approach, *Water Resour. Res.*, *48*, W11524, doi:10.1029/2012WR012319.
Inamdar, S., G. Dhillon, S. Singh, S. Dutta, D. Levia, D. Scott, M. Mitchell, J. Van Stan, and P. McHale (2013), Temporal variation in end-member chemistry and its influence on runoff mixing patterns in a forested, Piedmont catchment, *Water Resour. Res.*, *49*, 1828–1844, doi:10.1002/wrcr.20158.
Kendall, K. A., J. B. Shanley, and J. J. McDonnell (1999), A hydrometric and geochemical approach to test the transmissivity feedback hypothesis during snowmelt, *J. Hydrol.*, *219*, 188–205, doi:10.1016/S0022-1694(99)00059-1.
Kendall, S., and E. A. Caldwell (1998), Fundamentals of isotope geochemistry, in *Isotope Tracers In Catchment Hydrology*, edited by C. Kendall and J. J. McDonnell, pp. 51–86, Elsevier, Amsterdam.
Liu, F., M. W. Williams, and N. Caine (2004), Source-waters and flow paths in an alpine catchment, Colorado Front Range, United States, *Water Resour. Res.*, *40*, W09401, doi:10.1029/2004WR003076.
Lott, D. A., and M. T. Stewart (2012), A power function method for estimating base flow, *Ground Water*, *51*, 442–451, doi:10.1111/j.1745-6584.2012.00980.x.
Magilligan, F. J., and K. H. Nislow (2005), Change in hydrologic regime by dams, *Geomorphology*, *71*, 61–78, doi:10.1016/j.geomorph.2004.08.017.
McNamara, J. P., D. L. Kane, and L. D. Hinzman (1997), Hydrograph separations in an Arctic watershed using mixing model and graphical techniques, *Water. Resour. Res.*, *44*, 1707–1719, doi:10.1029/97WR01033.
Nathan, R. J., and T. A. McMahon (1990), Evaluation of automated techniques for base flow and recession analysis, *Water Resour. Res.*, *26*, 1465–1473, doi:10.1029/WR026i007p01465.
Pellerin B. A., W. M. Wollheim, X. Fend, and C. J. Vörösmarty (2007), The application of electrical conductivity as a tracer for hydrograph separation in urban catchments, *Hydrol. Processes*, *22*, 1810–1818, doi:10.1002/hyp.6786.
Pinder G. F., and J. F. Jones (1969), Determination of the ground-water component of peak discharge from the chemistry of total runoff, *Water Resour. Res.*, *5*, 438–44, doi:10.1029/WR005i002p00438.
Poff, N. L., J. D. Olden, D. M. Merritt, and D. M. Pepin (2007), Homogenization of regional river dynamics by dams and global biodiversity implications, *Proc. Natl. Acad. Sci. U. S. A.*, *104*, 5732–5737, doi:10.1073/pnas.0609812104.
Sanford, W. E., D. L. Nelms, J. P. Pope, and D. L. Selnick (2011), Quantifying components of the hydrologic cycle in Virginia using chemical hydrograph separation and multiple regression analysis, *U.S. Geol. Surv. Sci. Invest. Rep., 2011–5198*, 78 pp.
Santhi, C.P., P. M. Allen, R. S. Muttiah, J. G. Arnold, and P. Tuppad (2008), Regional estimation of base flow for the conterminous United States by hydrologic landscape regions, *J. Hydrol.*, *351*, 139–153, doi:10.1016/j.jhydrol.2007.13.018.
Schaffrath, K. R. (2012), Surface-water salinity in the Gunnison River Basin, Colorado, water years 1989 through 2007, *U.S. Geol. Surv. Sci. Invest. Rep., 2012–5128*, 47 pp.
Sklash, M. G., and R. N. Farvolden (1979), The role of groundwater in storm runoff, *J. Hydrol.*, *43*, 45–65, doi:10.1016/S0167-5648(09)70009-7.
Stanton, J. S., S. M. Peterson, and M. N. Fienen (2010), Simulation of groundwater flow and effects of groundwater irrigation on stream base flow in the Elkhorn and Loup River Basins, Nebraska, 1895–2055: Phase Two, *U.S. Geol. Surv. Sci. Invest. Rep., 2010–5149*, 78 pp.
Stewart, M., J. Cimino, and M. Ross (2007), Calibration of baseflow separation methods with streamflow conductivity, *Ground Water*, *45*, 17–27, doi:10.1111/j.1745-6584.2006.00263.x.
Stottlemyer, R. S., and C. A. Troendle (1999), Effect of subalpine canopy removal on snowpack, soil solution, and nutrient export, Fraser Experimental Forest, CO, *Hydrol. Processes*, *13*, 2287–2299.
Stottlemyer, R. (2001), Processes regulating watershed chemical export during snowmelt, Fraser Experimental Forest, Colorado, *J. Hydrol.*, *245*, 177–195, doi:10.1016/S0022-1694(01)00342-3.
Sueker, J. K., J. N. Ryan, C. Kendall, and R. D. Jarrett (2000), Determination of hydrologic pathways during snowmelt for alpine/subalpine basins, Rocky Mountain National Park, Colorado, *Water Resour. Res.*, *36*, 63–75, doi:10.1029/1999WR900296.
Uhlenbrook, S., M. Frey, C. Leibundgut, and P. Maloszewski (2002), Hydrograph separations in a mesoscale mountainous basin at event and seasonal timescales, *Water Resour. Res.*, *38*(6), 1096, doi:10.1029/2001WR000938.
U.S. Bureau of Reclamation (2012), Colorado River Basin water supply and demand study, study report, 95 pp., U.S. Dep. of the Inter., Washington, D. C. [Available at http://www.usbr.gov/lc/region/programs/crbstudy/finalreport/studyrpt.html.]
Wagner, R. J., R. W. Boulger Jr., C. J. Oblinger, and B. A. Smith (2006), Guidelines and standard procedures for continuous water-quality monitors-Station operation, record computation, and data reporting, *U.S. Geol. Surv. Tech. Meth., 1-D3*, 51 pp.
Wahl, K. L., and T. L. Wahl (1988), Effects of regional ground water declines on streamflows in the Oklahoma Panhandle, in Proceedings of Symposium on Water-Use Data for Water Resource Management, pp. 239–249, Am. Water Resour. Assoc., Tucson, Ariz.
Wigley, T. M. L., and P. D. Jones (1985) Influences of precipitation changes and direct CO_2 effects on streamflow, *Nature*, *314*, 149–152, doi:10.1038/314149a0.
Williams, M. W., and J. M. Melack (1991), Precipitation chemistry in and ionic loading to an alpine basin, Sierra Nevada, *Water Resour. Res.*, *27*, 1563–1574, doi:10.1029/90WR02773.
Winter, T. C., J. W. Harvey, O. L. Franke, and W. M. Alley (1998), Ground water and surface water: A single resource, *U.S. Geol. Circ., 1139*, 79 pp.
Wolock, D. M. (2003), Base-flow index grid for the conterminous United States, *U.S. Geol. Surv. Open File Rep., 03-263*.